

Static Modeling of an Inflatable Robotic Arm for Aerospace Applications

Original

Static Modeling of an Inflatable Robotic Arm for Aerospace Applications / Troise, M., Gaidano, M., Palmieri, P., Ruggeri, A., Mauro, S.. - ELETTRONICO. - 120:(2022), pp. 298-305. (RAAD 2022: the 31st International Conference on Robotics in Alpe-Adria Danube Region Klagenfurt am Wörthersee (Austria) 8-10 June 2022) [10.1007/978-3-031-04870-8_35].

Availability:

This version is available at: 11583/2962195 since: 2022-04-28T18:20:25Z

Publisher:

Springer, Cham

Published

DOI:10.1007/978-3-031-04870-8_35

Terms of use:

This article is made available under terms and conditions as specified in the corresponding bibliographic description in the repository

Publisher copyright

(Article begins on next page)

Static modeling of an inflatable robotic arm for aerospace applications

Mario Troise✉, Matteo Gaidano, Pierpaolo Palmieri,
Andrea Ruggeri, and Stefano Mauro

Department of Mechanical and Aerospace Engineering, Politecnico di Torino,
C.so Duca degli Abruzzi 24, 10129, Torino, Italy
{mario.troise, matteo.gaidano, pierpaolo.palmieri,
andrea.ruggeri, stefano.mauro}@polito.it

Abstract. Robots designed with soft material represent a growing trend in recent years and their use in space applications could minimize bulk and mass, reducing space mission costs. To achieve this goal the structure of soft robots must guarantee the possibility to be stored using deployment mechanisms. In this paper, the concept of an innovative inflatable robotic arm is proposed. The robot consists of two inflatable links and three actuated rigid joints. It can be stored in a relatively small package, if compared to its extended configuration, and can be inflated when required. After an overview of the robotic system, a radial deformation model is proposed to describe the link behavior, aiming for developing its control. The last section shows experimental tests performed on the link prototype to evaluate the static characterization with respect to the supplied pressure. Results suggest the validity of the adopted approach to model the inflatable link, putting the basis for the development of a suited control algorithm for the robotic system.

Keywords: Soft robotics, inflatable structures, characterization, deformation model, space robotics, manipulators

1 Introduction

In industrial environments, traditional robot manipulators are essential to accomplish many tasks, while robotic technologies begin to be essential in space applications [1]. Industrial robots can generate high contact forces, achieving desired tasks with great accuracy and repeatability. However, these manipulators are relatively bulky and heavy that is a disadvantage if embarked on space vehicles. Typically space applications require specifically designed robots, with a special attention to mass and encumbrance in retracted position.

Robots designed with soft material are a growing trend in recent years and they could better fit the requirements in space exploration permitting to resolve aerospace issues. Soft robots can be suitable for on-board, as robotic assistants, and for off-board applications, as berthing activity or space debris collection. Their design can be gathered into two categories, articulated [2] and continuum robots [3]. Furthermore, they can

span along all the spectrum between totally soft and rigid structures [4]. The links of articulated manipulators can be inflatable, guaranteeing the possibility to be stored in a limited volume, and the joints can be rigid [5], soft [6] or with variable stiffness [7]. However, the use of soft joints significantly reduces the load capacity of the robot.

In the last years, the development of collaborative robot and collision avoidance algorithms [8], [9], [10], [11] has increased the chances for a successful Human-Robot Collaboration (HRC) [12]. However, robots with intrinsic soft structure can improve safety in the event of an undesired collision, since the soft structure has the effect of buffering energy during a collision allowing a safer HRC [13]

In literature inflatable link has been described in several methods: in [14] the authors used pseudo-rigid body model to extract its bending stiffness, in [15] a vision sensor was placed inside the link to provide information about the structural deformation and, in [16] the stiffness and maximum load values of inflatable cylindrical tubes under different inflation pressures was obtained.

The design of soft manipulators influences the choice of the control strategy and dynamic parameters are crucial for the design an efficient controller, their identification is possible through appropriate algorithms [17] and considering the effects of temperature and mounting configuration [18]. However, in typically space applications the movements of the robots are very slow and to control them a quasi-static approach can be considered.

This paper presents a static model to account the deformation of a novel space robotic arm, consisting in inflatable links and electric actuation. This work distinguishes from the state of the art since it describes the bending stiffness of inflatable links considering their radial deformations due the air pressure level. Radial deformation model allows taking into account the variation of the moment of inertia as function of air pressure supply, improving the estimate of bending stiffness of the robot. Results suggest the validity of the deformation model and they will be used to improve the control algorithm showed in [19], and sensor and control strategy showed in [20].

2 Robotic system

The anthropomorphic soft arm consists in three revolute joints and two inflatable links. The links, made of a soft material, have rigid cups that guarantee to be connected with joints allowing them to assume a cylindrical shape when inflated. The structure of the extended configuration is shown in Fig. 1. The links are designed according to considerations discussed in previous work [21] about the influence of the internal pressure and the radius on the performances. The joint structural part hosts the motors and will be fabricated throughout additive manufacturing techniques, minimizing the weight and guaranteeing the resistance to loads at the same time. In order to save space on the stowing bay, soft manipulator can be deflated and stored in a relatively small package. A pneumatic line is responsible to control the inflation and deflation stages. Once reached the deployed configuration, the pneumatic supply is cut off and the robot is ready for the working phase. However, the using of inflatable links entail non-negligible deformations related to the robot payload. Defining the correlation between the

force applied on the link and the generated deformation would allow to increase the performance of the robot control system.

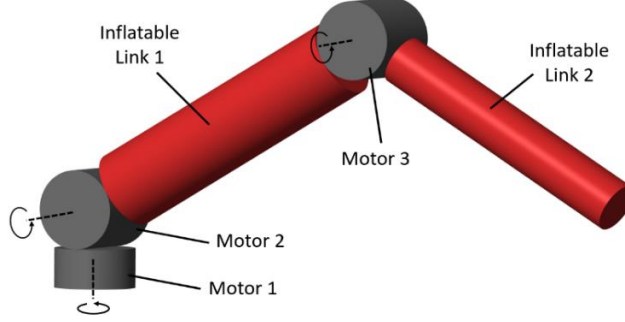


Fig. 1. Functional scheme of the anthropomorphic inflatable robot

3 Deformation model

Since links are maintained stressed by the pressure they are modeled as a rigid beam until the moment acting on them reaches the wrinkling moment. In literature, several expressions are used to define the wrinkling moment [22] [23] [24]; in this work the Veldman's model [22] has been chosen. The contribution of the material and membranes has been considered combining the Wielsgosz [23] and Wood [24] models with an adaptation for orthotropic materials. The first term is the same as that proposed by Wielsgosz and represents the membrane contribution, while the second is an adaptation of the Wood's model. The expression of wrinkling moment M_{wr} are reported below:

$$M_{wr} = \frac{1}{2} \left(\frac{\pi}{2} \right)^2 p r^3 + \frac{1}{2} \frac{2\sqrt{2}}{9} E_x \pi r t^2 \sqrt{\frac{E_\theta}{E_x} \sqrt{\frac{1}{1 - \nu_{x\theta} \nu_{\theta x}} + 4 \cdot \frac{p}{E_\theta} \left(\frac{r}{t} \right)^2}} \quad (1)$$

where p is the internal link pressure, r is radius of the link, ν is the Poisson coefficient, t is the thickness of the link, E_x and E_θ are the longitudinal and torsional Young's modules. The deflection of an inflatable beam, below the wrinkling moment, can be determined using analogous expression to the case of a rigid beam:

$$f = Q \cdot \frac{L^3}{3 \cdot E_x \cdot I} \quad M < M_{wr} \quad (2)$$

where Q is the applied load, I is the moment of inertia and L the length. The deflection would appear independent of the inflation pressure. Furthermore, the mechanical properties of each links are unknown because the value of longitudinal Young's module can be different for the robot links, it must be determined through experimental tests. To improve the accuracy of the inflatable link model the influence of internal pressure on the deflection is introduced. When the robot is inflated the internal pressure radially

deforms the link leading to a variation of its moment of inertia. The expression of radial deformation produced by internal pressure is reported below:

$$u = \rho \left[(1 - \nu) + \frac{1}{\rho^2} (1 + \nu) \right] \cdot \frac{\beta^2}{1 - \beta^2} \cdot \frac{r \cdot p_i}{E_x} \quad (3)$$

$$\begin{cases} R_e = r_e + u(r_e) \\ R_i = r_i + u(r_i) \end{cases} \quad (4)$$

$$\begin{cases} R_m = \frac{(R_e + R_i)}{2} \\ t' = R_e - R_i \end{cases} \quad (5)$$

where u is the radial deformation, E_x is the Young's modulus, r is the radius value in a generic surface point, r_e is nominal external radius of the link, r_i is nominal internal radius of the link, ρ is the ratio between r and r_e , β is the ratio between r_e and r_i , R_e and R_i are the deformed external and internal radius. However, using a thin material sheet allows assuming that thin does not change because the radial deformation will be the same for both internal and external radius. Solving the following equation, the value of Young's modulus of the link is calculated:

$$E_x = \frac{L^3}{3 \cdot I(p)} \cdot \frac{Q}{f} \quad (6)$$

4 Inflatable link prototype and experimental set-up

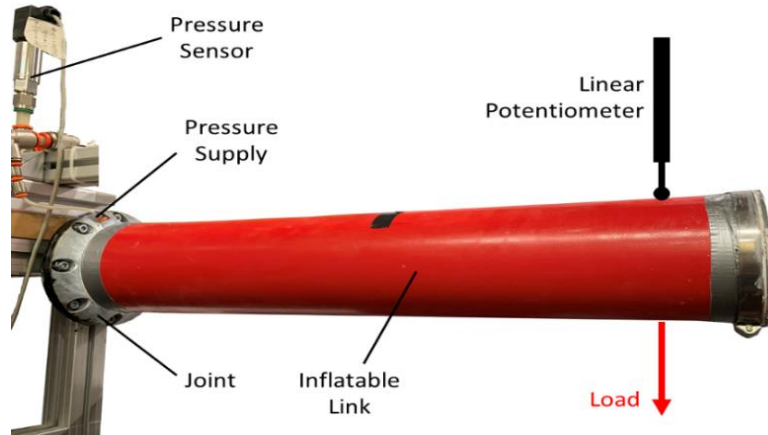


Fig. 2. Inflatable link prototype and experimental set-up of the static tests

A prototype of the inflatable link has been made by rolling and gluing a flexible PVC sheet, obtaining a cylindrical shape and good air pressure resistance. The link is connected to the test bench with screws. On the plug, a hole for the pressure supply is present. The pressure can be regulated with a pressure reducing valve. The link has length $L = 600$ mm, radius $r = 55$ mm and wall thickness $t = 0.5$ mm. During the tests, the bending load is applied using calibrated weights at a known position, $d = 470$ mm. The deflection has been measured using a resistive potentiometer at the application's point of the load. Then, a map with deflections and applied forces is built. The experimental set-up of the static test is shown in Fig. 2. The pressure is maintained constant during the test using a pressure regulator and measured using a pressure sensor.

5 Results

During the static tests, for each level of internal pressure, a load has been added till the collapse of the structure. The static characteristic of the link can be built using the data obtained from the tests. Results are shown in Fig. 3.

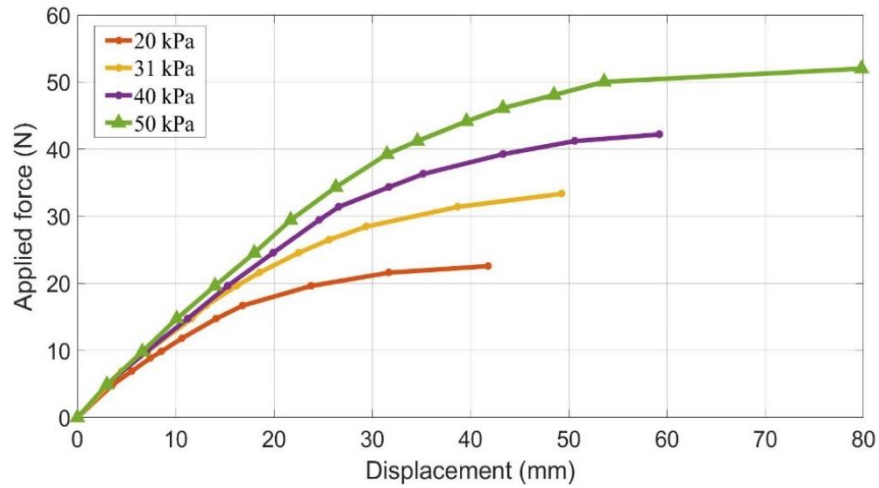


Fig. 3. Static characteristic of the link prototype depending on the internal pressure level

Fig. 3 was built using average data obtained carrying out several tests for each level of pressure in which the application point of the load is the same, when the wrinkling moment occurs the applied force significantly does not change as the displacement increases. In Table 1 both the average value and variance of Young's modulus using radial deformation model are reported.

Table 1. Average value and variance of Young modulus with the radial deformation model

	20 kPa	31 kPa	40 kPa	50 kPa
\bar{E}_x	164	182	177	182
$\sqrt{\sigma_E^2}$	12.0	17	21	14

Where \bar{E}_x and $\sqrt{\sigma_{E_x}^2}$ are the average value and variance of Young's modulus for each level of pressure. Table 1 has been obtained carrying out several tests for each level of pressure. For each of them, the radial deformations of the link, using Eq. 3, have been estimated and, they have been used to calculate the average value and variance of Young's modulus. The use of the radial deformation model allows changing the moment of inertia when the pressure changes, achieving the description of the slope of the experimental curves using the Veldman's model, as showed in Fig. 4 and Fig. 5.

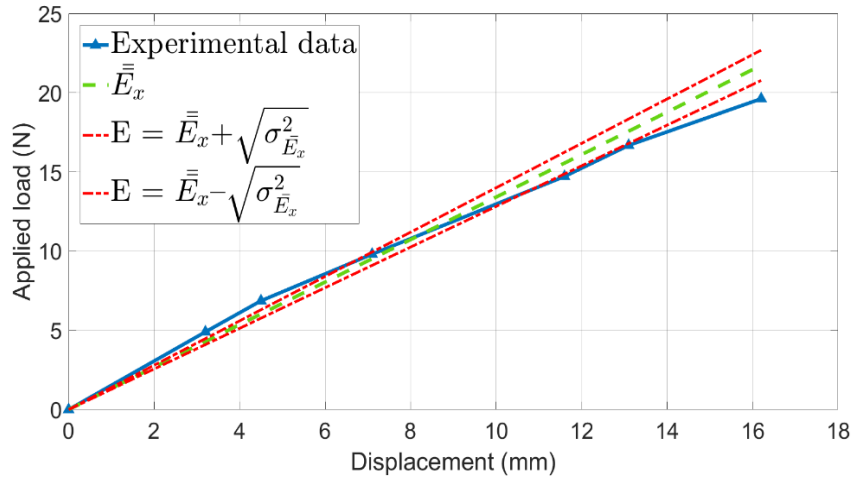


Fig. 4. Comparisons between Veldman's model with radial deformation and experimental static characteristics, $p = 31 \text{ kPa}$

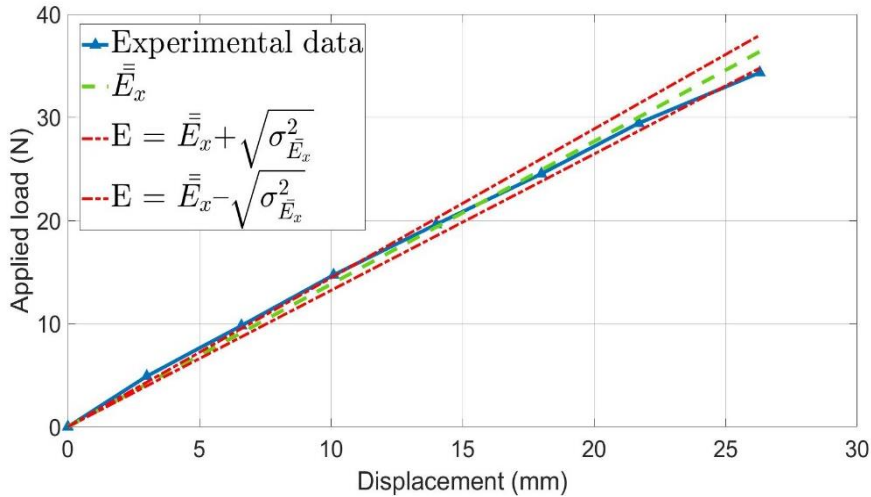


Fig. 5. Comparisons between Veldman's model with radial deformation and experimental static characteristics, $p = 50 \text{ kPa}$

6 Conclusion

This paper presented a model to account the deformation of a novel inflatable robot for space applications. The robot has two inflatable links and three revolute joints, it can be enclosed in a package and deployed when required. The model of the radial deformations of the links due to the air pressure was discussed. Radial deformation model allowed taking into account the variation of the moment of inertia as function of air pressure supply. The prototype of the inflatable link was built and statically characterized. Using a radial deformation model to describe inflatable link allows determining its Young's module for any pressure value, without discretizing the experimental curves. Results proved the validity of the model proposed and, the load capacity of the inflatable link has been proven compatible with the typical space loads requirements. Further works will focus on the realization of the overall system and on the development of a dynamic model. The radial deformation model will be used to improve load and pose estimation algorithms, described in [19]. Moreover, control algorithms should be implemented using appropriate sensors and sensor fusion strategies. Collision avoidance and hand-following algorithms should be tested for HRC applications

References

- [1] Bogue, R.: The growing use of robots by the aerospace industry. *Industrial Robot: An International Journal*, (2018).
- [2] Gillespie, M. T., Best, C. M., Killpack, M. D.: Simultaneous position and stiffness control for an inflatable soft robot. *IEEE international conference on robotics and automation (ICRA)*, IEEE, (2016).
- [3] Giannaccini, M. E., et al.: Novel Design of a Soft Lightweight Pneumatic Continuum Robot Arm with Decoupled Variable Stiffness and Positioning. *Soft Robotics*, vol. 5(1), (2018).
- [4] Hughes, J., et al.: Soft Manipulators and Grippers: A Review. *Frontiers in Robotics and AI*, vol. 3, (2016),
- [5] Kim, H. J. Kawamura, A., Nishioka, Y., Kawamura, S.: Mechanical design and control of inflatable robotic arms for high positioning accuracy. *Advanced Robotics*, vol. 32(2), (2018).
- [6] Palacio, J. M. A., Riwan, A., Mechbal, N., Monteiro, E., Voisebert, S.: A novel inflatable actuator for inflatable robotic arms. *IEEE International Conference on Advanced Intelligent Mechatronics (AIM)*. IEEE, (2017).
- [7] Mengacci, R., et al.: On the motion/stiffness decoupling property of articulated soft robots with application to model-free torque iterative learning control. *The International Journal of Robotics Research*, vol. 40(1), (2021).
- [8] Mauro, S., Scimmi, L. S., Pastorelli, S.: Collision avoidance algorithm for collaborative robotics. *International Journal of Automation Technology* vol. 11.(3) (2017).
- [9] Scimmi, L. S., Melchiorre, M. Mauro, S., Pastorelli, S.: Multiple collision avoidance between human limbs and robot links algorithm in collaborative tasks. *ICINCO*, (2018).
- [10] Scimmi, L. S., Melchiorre, M. Mauro, S., Pastorelli, S.: Implementing a Vision-Based

- Collision Avoidance Algorithm on a UR3 Robot. 23rd International Conference on Mechatronics Technology (ICMT), IEEE, (2019).
- [11] Melchiorre, M., Scimmi, L. S., Pastorelli, S., Mauro, S.: Collision Avoidance using Point Cloud Data Fusion from Multiple Depth Sensors: A Practical Approach. 23rd International Conference on Mechatronics Technology (ICMT). IEEE, (2019).
- [12] Scimmi, L. S., Melchiorre, M., Troise, M., Mauro, S., Pastorelli S.: A practical and effective layout for a safe human-robot collaborative assembly task. *Applied Sciences*, vol. 11(4), (2021).
- [13] Pang, G., et all.: Development of flexible robot skin for safe and natural human-robot collaboration. *Micromachines*, vol.9(11), (2018).
- [14] Sanan, S., Moidel, J. B., Atkeson, C. G.: Robots with inflatable links. *IEEE/RSJ International Conference on Intelligent Robots and Systems*. IEEE, (2009).
- [15] Oliveira, J., Ferreira, A., Reis, J. C. P.: Design and experiments on an inflatable link robot with a built-in vision sensor. *Mechatronics*, vol. 65, (2020).
- [16] Okda, S., Akl, W., Elsabbagh, A.: Structural behaviour of inflatable PVC fabric cylindrical tubes. *IOP Conference Series: Materials Science and Engineering*, vol. 610(1) (2019).
- [17] Raviola, A., De Martin, A., Guida, R., Pastorelli, S., Mauro, S., Sorli, M.: Identification of a UR5 collaborative robot dynamic parameters. *International Conference on Robotics in Alpe-Adria Danube Region*. Springer, Cham, (2021).
- [18] Raviola, A., De Martin, A., Guida, R., Pastorelli, S., Mauro, S., Sorli, M.: Effects of temperature and mounting configuration on the dynamic parameters identification of industrial robots. *Robotics*, vol. 10(3), (2021).
- [19] Troise, M., Gaidano, M., Palmieri, P., Mauro, S.: Preliminary Analysis of a Lightweight and Deployable Soft Robot for Space Applications. *Applied Sciences*, vol. 11(6), (2021).
- [20] Palmieri, P., Gaidano, M., Ruggeri, A., Salamina, L., Troise, M., Mauro, S.: An Inflatable Robotic Assistant for Onboard Applications. *72nd IAC 2021, Dubai, UAE*, (2021).
- [21] Palmieri, P., Gaidano, M., Ruggeri, A., Salamina, L., Troise, M., Mauro, S.: A deployable and inflatable robotic arm concept for aerospace applications. *2021 IEEE 8th International Workshop on Metrology for AeroSpace (MetroAeroSpace)*, IEEE, (2021).
- [22] Veldman, S. L., Bergsma, O. K., Beukers, A.: Bending of anisotropic inflated cylindrical beams. *Thin-walled structures*, vol. 43(3), (2005).
- [23] Wielgosz, C., Thomas, J. C.: Deflections of inflatable fabric panels at high pressure. *Thin-Walled Structures*, vol. 40(6), (2002).
- [24] Wood, J.: The flexure of a uniformly pressurized, circular, cylindrical shell. *Journal of Applied Mechanics*. vol. 25(12), (1958).